The Journal of Chemical Physics

A thermodynamic model of contact angle hysteresis

Cite as: J. Chem. Phys. **147**, 064703 (2017); https://doi.org/10.1063/1.4996912
Submitted: 22 May 2017 • Accepted: 18 July 2017 • Published Online: 11 August 2017

Lasse Makkonen

A thermodynamic model of contact angle hysteresis

Lasse Makkonen[a)]
VTT Technical Research Centre of Finland, Espoo 02044 VTT, Finland

(Received 22 May 2017; accepted 18 July 2017; published online 11 August 2017)

When a three-phase contact line moves along a solid surface, the contact angle no longer corresponds to the static equilibrium angle but is larger when the liquid is advancing and smaller when the liquid is receding. The difference between the advancing and receding contact angles, i.e., the contact angle hysteresis, is of paramount importance in wetting and capillarity. For example, it determines the magnitude of the external force that is required to make a drop slide on a solid surface. Until now, fundamental origin of the contact angle hysteresis has been controversial. Here, this origin is revealed and a quantitative theory is derived. The theory is corroborated by the available experimental data for a large number of solid-liquid combinations. The theory is applied in modelling the contact angle hysteresis on a textured surface, and these results are also in quantitative agreement with the experimental data. [http://dx.doi.org/10.1063/1.4996912]

INTRODUCTION

Wetting of solid surfaces by a liquid is a classical and familiar physics problem and its understanding is crucial in many industrial processes.[1–5] When the liquid does not wet the solid completely, a specific Young's equilibrium angle[6] θ is formed at the three-phase contact line and can be used as a measure of the hydrophobicity of surfaces.[7,8]

However, wettability is not determined by θ alone. In addition, there is another important property, contact angle hysteresis, that characterizes wetting. Under the influence of an external force, such as gravity, no motion of the contact line occurs instantaneously but the contact angle changes. In the case of a drop, its shape then becomes asymmetric, and only when a sufficiently high force is exerted does the sliding begin (Fig. 1). At that time, there occurs the highest possible contact angle, θ_a, and the lowest possible contact angle, θ_r, the difference of which is called the contact angle hysteresis, $H = \theta_a - \theta_r$.[9,10] The effect of the contact angle hysteresis can also be measured by $\cos\theta_r - \cos\theta_a$, which is linked with the net force that is required to make a drop slide.[11]

Contact angle hysteresis is a crucially important element of wetting and, given the great practical importance of the subject, numerous experimental and theoretical studies have been made to understand it. These have been reviewed by de Gennes[8] and, more recently, by Eral *et al.*[12] Attempts have been made to explain the origin of contact angle hysteresis, e.g., by surface roughness and chemical heterogeneities, surface deformation, liquid adsorption and retention, viscous dissipation, molecular rearrangement upon wetting, and inter-diffusion (for review, see Ref. 12). Qualitatively, contact angle hysteresis has also been explained by the shape of the disjoining isotherms[13–15] and by a phenomenological phase field model.[16]

However, there is no consensus on the fundamental origin of contact hysteresis on a smooth and homogenous surface, and there is no well-verified quantitative theory. Most of the present models predict no contact angle hysteresis on a smooth chemically homogenous surface, while experimentally hysteresis is always observed, even on inherently smooth surfaces.[17,18] Eral *et al.*[12] end their review by stating "The manifestations of contact angle hysteresis are everywhere in our daily lives, yet how to include this physical phenomenon in models is far from settled."

Here, the fundamental origin of contact angle hysteresis is revealed and a thermodynamic quantitative theory is developed for an ideal surface. The theory is then extended to textured surfaces.

THE FUNDAMENTALS

At the heart of the problem is the balance at a contact line proposed by Thomas Young[10] in 1805. Formally, Young's idea results in the following equation:

$$\gamma_{SV} = \gamma_{SL} + \gamma_{LV}\cos\theta, \tag{1}$$

where γ_{SV}, γ_{SL}, and γ_{LV} are, respectively, the solid-vapor (S,V), solid-liquid (S,L), and liquid-vapor interfacial tensions (Fig. 2). In this classical construction, the three mechanical surface tensions γ_{SV}, γ_{SL}, and γ_{LV} are at equilibrium in the direction parallel to the solid surface.

Equation (1) has widely not only been interpreted as the mechanical balance of the three surface tensions but also as the result of minimizing the total free energy. In the latter interpretation, γ_{SV}, γ_{SL}, and γ_{LV} in Fig. 2 represent scalar thermodynamic surface energies instead of mechanical tension vectors. While the surface tensions involving a liquid phase can be interpreted either way, the mechanical surface

a)Author to whom correspondence should be addressed: lasse.makkonen@vtt.fi

FIG. 1. Drops of water sliding on an inclined polymer surface.

tension of a dry solid is a contentious concept.[19–21] Nevertheless, Eq. (1) can be used when considering the balance of forces solely in parallel to the solid surface because such equilibrium must exist irrespectively of the origin and nature of the forces.

A consequence of Young's equilibrium is that a drop on a solid surface, or a column of liquid in a thin capillary, should move even with the slightest external force. Historically, this is referred to as the Bertrand theorem. However, a contact line is pinned, so when one tries to move a drop or a liquid column, Eq. (1) is violated. Joanny and de Gennes[22] in 1984 started their analysis on contact angle hysteresis by writing that "the natural interpretation of this violation is based on irregularities of the solid surface." This idea found its way into textbooks[3] and has been subsequently adopted to the extent that even in the most recent literature, phrases such as "... known to originate from surface heterogeneities ..." are used when discussing the physics of contact angle hysteresis.[23]

It is shown in the following that this idea is incorrect. This is not to say that surface heterogeneities could not cause contact angle hysteresis but that the fundamental origin of contact line pinning and contact angle hysteresis lays elsewhere. That it was overlooked by Joanny and de Gennes[22] and all subsequent authors is rather peculiar because the physics here are embedded in the most basic definition of the Gibbsian surface thermodynamics: *Work must be spent when creating new surface*, and this work defines the thermodynamic surface energy γ (J m^{-2}). Specifically, the International Union of Pure and Applied Chemistry (IUPAC) definition of surface tension reads as follows: "Work required to increase a surface area

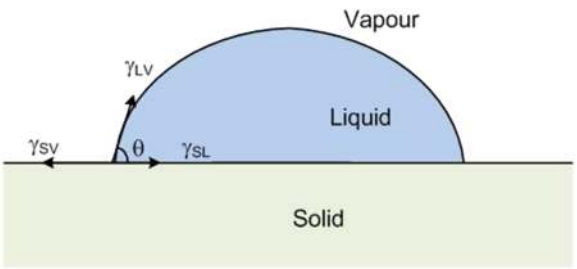

FIG. 2. Young's construction of surface tensions at a three-phase contact line of a drop.

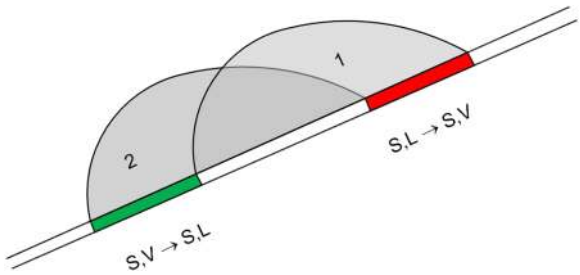

FIG. 3. Example of creating a new interface. Upon sliding of a drop, the solid-vapor (S,V) interface disappears and a solid-liquid (S,L) interface forms at the advancing contact line. Correspondingly, the solid-liquid interface disappears and a solid-vapor surface is formed at the receding contact line.

divided by that area. When two phases are studied, it is often called interfacial tension."

Obviously, when a three-phase contact recedes along the solid surface, a new solid surface is created behind the contact line. Correspondingly, when a contact line advances, a new solid-liquid interface is created behind it. These processes are illustrated in Fig. 3 by a sliding drop in the ideal case where the advancing and receding contact lines move simultaneously at the same velocity.

One could argue that the surface energy of the disappearing surface would be available as free energy on the other side of the contact line. In that case, the frictional force F would be related to the difference of the solid and solid-liquid interface energies. However, the surface energy is a thermodynamic concept, and in thermodynamic theory, the surface energy is not associated with a volume but with a two-dimensional discrete interface. Therefore, when a contact line moves across a solid surface, the surface energy of a disappearing surface is not stored in any way and thus cannot be transferred to the other side of the contact line. Consequently, upon the motion of a three-phase contact line, the surface energy of the disappearing surface dissipates into thermal energy.

Therefore, *work must be done in moving the contact line*. This is possible only when there is a frictional force F, against which work is done. The magnitude of this frictional force F is such that the related tension F/w equals the thermodynamic surface energy γ of the interface being created. This is directly measurable, e.g., when stretching a liquid film. In the general case, this can be understood by considering an object of width w moving in complete contact by an increment dx so that an area dA is formed behind it. Then, work dE is spent in creating a new surface. It follows from the definition of force that $F = dE/dx = \gamma dA/dx = \gamma w$. Thus, the frictional tension that resists the motion is

$$F/w = \gamma. \tag{2}$$

CONTACT ANGLE HYSTERESIS ON AN IDEAL SOLID SURFACE

As shown by Eq. (2), when a new smooth interface is formed, the resisting frictional tension F/w equals the surface energy γ of that interface. Consequently, when the contact line on the left side of Fig. 3 is forced to advance to the left, thus creating a new solid-liquid interface, the frictional tension that

resists the motion equals γ_{SL}. A force balance parallel to the solid surface must exist in this situation. The frictional tension is in addition to the tensions that exist already in the static equilibrium described in Fig. 2. To adjust the static force equilibrium in Eq. (1) to the new dynamic situation, the additional frictional tension arising at the continuously moving contact line F/w = γ_{SL} must be balanced by a change in the contact angle, i.e.,

$$\gamma_{SL} = \gamma_{LV}(\cos\theta - \cos\theta_a). \tag{3}$$

The change occurs in the contact angle because it is the only free parameter in the system, the other parameters, i.e., surface energies, being material constants. Equation (3) is analogous to the concept of spreading tension,[22] which, in a quasi-static condition, equals the frictional tension. When using Eq. (1), the force equilibrium at an advancing contact line becomes

$$\gamma_{SV} = \gamma_{SL} + \gamma_{LV}\cos\theta_a + \gamma_{SL}, \tag{4}$$

where θ_a is the advancing contact angle.

Similarly, when considering the receding contact line, i.e., the situation where in Fig. 3 the left side of the drop moves to the right, the motion brings in an additional frictional tension, γ_{SV}, owing to the work spent in creating a new solid-vapor interface at the contact line. This must be balanced by the change in the contact angle so that

$$\gamma_{SV} = \gamma_{LV}(\cos\theta_r - \cos\theta). \tag{5}$$

The force equilibrium at the receding contact line is thus obtained as

$$\gamma_{SV} + \gamma_{SV} = \gamma_{SL} + \gamma_{LV}\cos\theta_r, \tag{6}$$

where θ_r is the receding contact angle.

The frictional terms on the left side of Eqs. (3) and (5) can also be interpreted by the conventional concept of the work of wetting. In a situation where the contact angle does not change upon moving, this work is that of immersional wetting $W_i = \gamma_{SV} - \gamma_{SL}$. Accordingly, when considering the motion of a contact line as an irreversible process, W_i equals either $-\gamma_{SL}$ as in Eq. (3) or $-\gamma_{SV}$ as in Eq. (5), depending on the direction of the motion.

Equations (4) and (6) provide a thermodynamic model of the dynamic contact angles on a smooth and homogenous surface as a function of the surface energies of the system. These equations include two material properties, γ_{SV} and γ_{SL}, that cannot be directly measured. However, γ_{SV} and γ_{SL} can be related to the static equilibrium contact angle θ as will be discussed below.

Berthelot's rule[24] follows from applying the geometric mean combination rule in the London theory of dispersion forces. Thus, it has a theoretical basis in the case of non-polar materials.[25] However, because of entropic contributions[26] and non-dispersive forces across interfaces, Berthelot's rule needs to be modified so that a semi-empirical interfacial interaction parameter ϕ is used.[27] Then, the solid-liquid interface energy can be expressed as

$$\gamma_{SL} = \gamma_{SV} + \gamma_{LV} - 2\phi(\gamma_{SV}\,\gamma_{LV})^{1/2}. \tag{7}$$

This Girifalco-Good equation is widely discussed in the literature. From Eqs. (1) and (7), it follows that

$$\gamma_{SV}/\gamma_{LV} = [(1+\cos\theta)/2\phi]^2. \tag{8}$$

Theory[27] and experiments[27,28] show that the value of the interfacial interaction parameter ϕ varies between 0.5 and 1.2.

Inserting Eq. (8) into Eqs. (4) and (6), respectively, and utilizing Eq. (1) give analytical expressions for the two dynamic contact angles as a function of the static contact angle. For the advancing contact angle

$$\cos\theta_a = [-\cos^2\theta + (8\phi^2 - 2)\cos\theta - 1]/4\phi^2. \tag{9}$$

The maximum contact angle is 180°, so that $\cos\theta_a$ has a limit, below which $\cos\theta_a = -1$ and H is determined by θ_r alone. For $\phi = 1$, the limit is at $\cos\theta = -0.464$ ($\theta = 117.7°$).

For the receding contact angle, the corresponding equation is

$$\cos\theta_r = [\cos^2\theta + (4\phi^2 + 2)\cos\theta + 1]/4\phi^2. \tag{10}$$

The minimum contact angle is 0°, so that $\cos\theta_r$ has a limit, above which $\cos\theta_r = 1$ and H is determined by θ_a alone. For $\phi = 1$, the limit is at $\cos\theta = 0.464$ ($\theta = 62.3°$).

It has been shown[28,29] that a linear relationship exists between the solid-liquid surface tension γ_{SL} and ϕ, i.e.,

$$\phi = -\alpha\gamma_{SL} + \beta. \tag{11}$$

In Eq. (11), α and β are the constants for a specific liquid. Their values have been determined both by studies based on contact angles and by direct measurements of liquid-liquid surface tensions.[28] These studies show that Eq. (11) provides a very high linear correlation coefficient for very different material combinations. From the applications point of view, water is the most important liquid, and for water-organic liquid systems, the correlation coefficient for Eq. (11) is 0.992 in the range ϕ = 0.5–1.0 of the data.[28]

One may utilize Eq. (11) by combining it with Eqs. (1) and (8) and solving for ϕ. This yields

$$\phi = \alpha\gamma_{LV}[\cos\theta - ((1+\cos\theta)/2\phi)^2] + \beta. \tag{12}$$

Thus, there is a theoretical solution for ϕ as a function of the static equilibrium contact angle θ. Inserting Eq. (12) into Eqs. (9) and (10) then gives us, for a system with known α and β, the equations for the dynamic contact angles θ_a and θ_r as a function of the static contact angle θ. These are third-degree equations and can readily be solved numerically.

RESULTS AND VALIDATION

According to the model developed above, for a liquid with known α and β, the dynamic contact angles θ_a and θ_r, as well as H, depend on θ alone. The theory explains the empirically observed basic features that the contact angle hysteresis is inherent to all surfaces and is independent of the contact line velocity[30] and the effective vertical force,[31] when viscosity effects and impurities can be excluded.

The results of the theory are shown in Fig. 4. The dependence of θ_a and θ_r on θ is shown in Fig. 4 making the assumption $\phi = 1$. In addition, the effect of the interfacial interaction parameter ϕ on the dynamic contact angles, as calculated by the theory, is illustrated in Fig. 4. Numerical solutions are shown in Fig. 4 for two liquids, water and ethylene glycol. They represent the highest and smallest mean

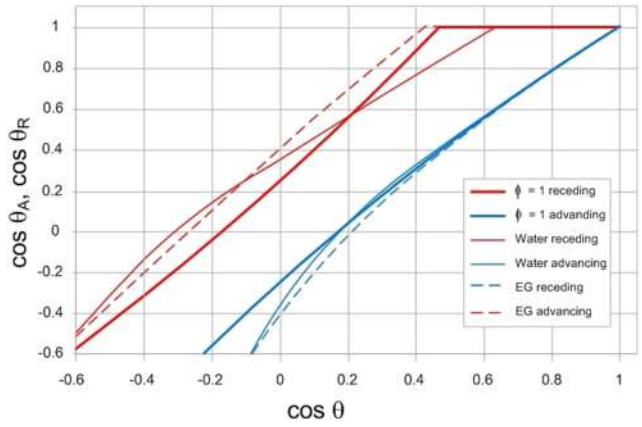

FIG. 4. Advancing (θ_a, blue) and receding (θ_r, red) contact angles as a function of the static contact angle as calculated by the theory for two liquids: water and ethylene glycol. The values used for parameters α and β are 0.0113 and 1.129 for water and 0.012 91 and 1.032 for ethylene glycol (EG).[28]

values of ϕ in the data based on direct liquid-liquid measurements.[28] The corresponding values of α and β are 0.0113 and 1.129 (water—organic liquid) and 0.012 91 and 1.032 (ethylene glycol—organic liquid).[28] Figure 4 shows that, although ϕ varies in a wide range, the dynamic contact angles are only moderately sensitive to deviations from the theoretical solution that assumes $\phi = 1$, i.e., $\alpha = 0$ and $\beta = 1$. The advancing contact angle θ_a is significantly affected by varying α and β within their experimental limits only at high contact angles.

Quantitative predictions of the theory, with the assumption that Berthelot's rule is valid in its original form, i.e., $\phi = 1$, are shown again in Fig. 5, where this theoretical prediction is compared with the available experimental data on the three contact angles from experiments on surfaces that have been considered "smooth" by the respective authors.[32–36]

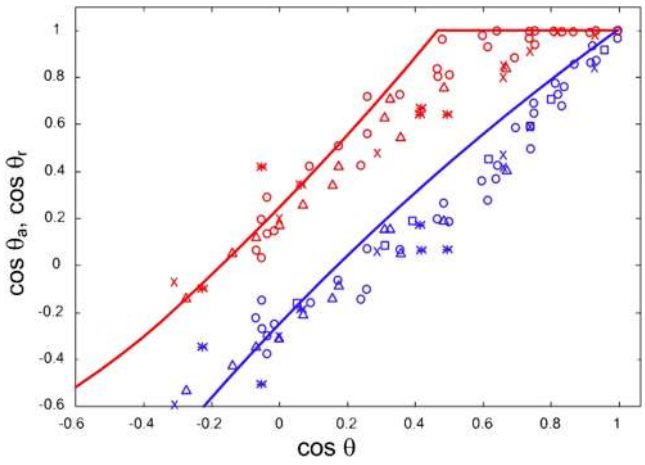

FIG. 5. Advancing (θ_a, blue) and receding (θ_r, red) contact angles as a function of Young's contact angle on a smooth surface, θ. The lines show the prediction of the theory with $\phi = 1$. The circles are the experimental data for water on plasma polymer surface coatings,[32] triangles for different water-ethanol mixtures on a Si_3N_4 surface,[33] squares for water on untreated and treated PET and PMS surfaces,[34] and stars for water on six other polymer surfaces.[35] The crosses are for different saturated hydrocarbon liquids on a PTFE surface.[36]

In view of Fig. 4, the scatter of the experimental data in Fig. 5 is undoubtedly caused by the material dependent variations in the interfacial interaction parameter ϕ. Minute roughness of the solids may also play a role here. Moreover, there are many inherent difficulties in determining the contact angles accurately, particularly determining the equilibrium state that corresponds to θ, and measuring θ_r at small angles.[37–41] This withstanding, the theory is in good quantitative agreement with the data. The data in Fig. 5 are based on four different measurement methods: the Wilhelmy immersion plate method, the capillary rise method, measuring the drop shape by pumping liquid in and out of a sessile drop, and the tilted plate method. The experiments include fifty different liquid-solid combinations plus one combination with 12 different liquid mixture concentrations. Hence, noting the uncertainty envelope shown in Fig. 4, the data in Fig. 5 provide strong support for the theory. Note that the model, as applied in Fig. 5, is purely physical, i.e., the curves in Fig. 5 include no fitting parameters or other experimental ingredients.

APPLICATION TO TEXTURED SURFACES

The model presented above for a smooth surface cannot be directly applied to a rough surface because the contact angles depend on the surface morphology at the contact line.[41–43] However, since the model represents the fundamental mechanism of contact angle hysteresis, it can be used as the foundation of any successful theory also on a rough surface. When applied to the Wenzel state on a textured surface, surface generation per increment dx is higher than on a smooth surface so that this theory gives $H^R = r\,H$. Here r is the ratio of the total surface area of the solid to its apparent surface area ($r > 1$). Thus, the model shows that increasing the roughness increases the contact angle hysteresis on a hydrophilic material, as experimentally observed.[44]

In the Cassie state, air is entrapped at the interface, and contact angles can be modeled by the differential Cassie fraction Φ_d, which is the solid fraction traversed by the contact line during a hypothetical small displacement.[33,45] The fraction Φ_d can be related to the conventional Cassie factor Φ_s, i.e., the ratio of the true solid-liquid contact area to the apparent interface area, when the surface texture morphology and the direction of the contact line motion in relation to it are known.[46,47] For the static contact angle θ^R on a textured pillar-like hydrophobic surface, the force balance in the Cassie-state can be formulated as[45]

$$\gamma_{LV}\cos\theta^R = \Phi_d(\gamma_{SV} - \gamma_{SL}) - (1 - \Phi_d)\gamma_{LV}. \qquad (13)$$

Analogously with Eqs. (4) and (6), the dynamic Cassie-Baxter equations become

$$\cos\theta_a{}^R = \Phi_{d,a}(1 + \cos\theta) - 1 - \Phi_{d,a}(\gamma_{SL}/\gamma_{LV}) \qquad (14)$$

for the advancing angle and

$$\cos\theta_r{}^R = \Phi_{d,r}(1 + \cos\theta) - 1 + \Phi_{d,r}(\gamma_{SV}/\gamma_{LV}) \qquad (15)$$

for the receding angle.

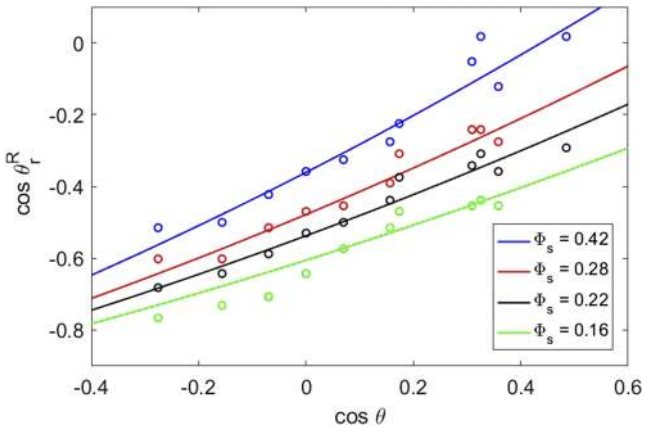

FIG. 6. Apparent receding contact angle on a textured surface θ_r^R vs. Young's equilibrium contact angle on a smooth surface θ. The points are experimental observations with different Cassie fractions Φ_s of rough surfaces consisting of micropillars.[33] The lines are predictions of this theory, Eq. (17).

Using Eqs. (1) and (8) and taking $\phi = 1$ for simplicity, these analytical solutions can be written as

$$\cos\theta_a^R = \Phi_{d,a}[(-\cos^2\theta + 6\cos\theta + 3)/4] - 1 \qquad (16)$$

and

$$\cos\theta_r^R = \Phi_{d,r}[(\cos^2\theta + 6\cos\theta + 5)/4] - 1. \qquad (17)$$

This allows purely theoretical modeling of the advancing and receding contact angles on a textured surface by variables Φ_d and θ.

The theoretical dynamic contact angles from Eqs. (16) and (17) can be compared with recent measurements of contact angle hysteresis on surfaces with a well-controlled Cassie fraction. Using the data for cylindrical pillars,[33] for which the differential solid fraction for the receding contact line is given[33] as $\Phi_{d,r} = (2/\pi^{1/2})\,\Phi_s^{1/2}$, the theory can be tested. This is presented in Fig. 6 for a geometry for which $\Phi_{d,a} = 0$.[46] Figure 6 shows excellent agreement for different Cassie fractions Φ_s, in a wide range of equilibrium contact angles.

DISCUSSION

The theory presented here has many important implications. From the theoretical point of view, it is now clear why the motion of a contact line is a dissipative process and involves a resisting frictional force. The existence of a frictional force, which causes contact angle hysteresis already on an ideal smooth surface, has been postulated[48–51] and measured[52] before but is identified and quantified here as the force that arises from creating a new surface behind a contact line. This mechanism is analogous with the thermodynamic origin of the sliding friction of solids.[53]

The resulting solution of the problem is remarkably simple in that the contact angle hysteresis H on a smooth and chemically homogenous surface depends only on Young's static equilibrium angle θ. Only for accurate estimates for polar materials does the interfacial interaction parameter ϕ need to be considered. This simplifies the characterization of surfaces where typically θ_a and θ_r have been measured but not θ. Since θ is generally considered more difficult to measure than the dynamic angles, application of this model will improve the accuracy of determining the static equilibrium Young's angle.

There has been a long debate on how the dynamic contact angles are related to the Young's equilibrium contact angle. Approximations $\theta = (\theta_a + \theta_r)/2$[54] and $\cos\theta = (\cos\theta_a + \cos\theta_r)/2$,[55] as well as some more complicated relationships,[56,57] have been proposed. Out of these, the analytical solution by Tadmor[56] is the most widely used.[58–61] The theory presented here shows that none of these proposals are accurate in the whole range of θ. More importantly, such approximations are no longer necessary since this theory provides the physical model of the problem. It turns out that θ is not a function of both θ_a and θ_r, but rather θ_a and θ_r are related to θ by two separate equations.

The theoretical results in Eqs. (9) and (10) reveal the fundamental difference between θ and θ_a. Consequently, θ_a or any measured static angle between θ and θ_a should not be used in Young's equation to replace θ, as done in some theories of contact angle hysteresis[62,63] and quite generally in determining solid surface energies by the advancing contact angle.

According to the theory presented here, the dynamic contact angles and the contact angle hysteresis are independent of the velocity of the contact line. This prediction is corroborated by the experimental data, which show that there is no velocity-dependence of dynamic contact angles for liquids with low viscosity.[30,64,65] Due to hydrodynamic effects, this theory is not directly applicable to viscous liquids moving at a high velocity or to a liquid with impurities.[66] Experimentally, contact angles have been studied at low velocities,[67] and the limit of the velocity dependence appears[30] to be at the viscosity of about 0.01 Ns/m^2. Therefore, this model is applicable to the issues of hydrophobicity in natural conditions.

In the medium range of θ, the data for both θ_a and θ_r appear to be systematically somewhat above the theoretical prediction in Fig. 5. In the receding case, errors in measuring θ_r are the most likely explanation for this.[32,36–39] There are many problems involved, such as deformation of the interfaces and varying fitting procedures of optical data,[67] particularly at small angles. In addition, liquid adsorption on the bulk material during the experiment[68] or a precursor film on the solid[69] may be factors here. In case of a drop at high contact angles, the mode of motion, i.e., sliding vs. rolling, does not explain the discrepancies in Fig. 5 because the thermodynamic cost of creating a new interface is unrelated to how the liquid moves.

Systematic errors in Fig. 5 may also arise due to difficulties in obtaining the true equilibrium when measuring the Young's static contact angle θ. These could be alleviated by a detailed statistical contact angle analysis.[67] Due to the pinning of the contact line, the apparent static contact angle may be far from θ, depending on the way the drop is placed on the surface, or when evaporation of the drop takes place. Apparently, an accurate value of θ may only be obtained by determining the most stable contact angle using tilted plane experiments.[35] More work is necessary in this area.

A related issue is that experimentally θ_a is increased and θ_r is decreased by noise.[70] The theory agrees with this observation since vibrations make the contact line move in both advancing and receding directions, thus reducing the larger apparent angle and increasing the smaller apparent angle. Large enough vibration levels mitigate hysteresis as predicted by the model and as experimentally observed.[70]

Yet another possible explanation for the systematic difference in θ_a in Fig. 5 is that the circles in the figure are based on the first immersion of the Wilhelmy plate method. On a slightly rough surface, the advancing angle is larger for the first immersion and remains at a smaller constant value thereafter.[71] This suggests that micro- or nano-bubbles of air are entrapped upon the first immersion, and that data based on subsequent immersion should be used in comparisons with the theory. Deviation from the symmetric drop shape in the tilted angle experiments does not significantly affect the measured contact angles,[72] but gravity may play a role.

In addition to experimental errors, one reason for the scatter in the data in Fig. 5 may be the varying stiffness of the solid materials. Some experiments suggest that H may be increased on compliant materials, such as natural rubber.[73] In view of the theory presented here, this is probably related to the elastic component of the surface energy of a soft solid, as described by the specific theories of wetting on deformable materials.[74–77] Surface restructuring of the bulk material may also play a role here, as some energy may be transferred across a moving contact line in that form. However, the effect of restructuring on the surface energy is generally quite small,[78] except perhaps for very soft materials.

The theoretical result that the contact angle hysteresis on a textured surface is a function of the equilibrium static contact angle θ measured on a smooth surface and the differential Cassie fraction Φ_d only makes the interpretation of hydrophobicity remarkably simpler. It also makes it possible to consider in detail the effect of specific surface texture geometries on contact angle hysteresis.[46,50] An increased slip length at very large micro-feature spacing may play a role in contact line dynamics.[79] However, no relationship between micro-feature scale and contact angle hysteresis, when the geometry and Cassie fraction are held constant, has been observed in the spacing range of 2–128 μm covered by the experiments.[46,80] Therefore, this theory is applicable to textured surfaces, at least in this range and when no precursor film is present.

SUPPLEMENTARY MATERIAL

See supplementary material for the experimental data in Fig. 5.

ACKNOWLEDGMENTS

This work was supported by the Academy of Finland, Grant No. 297278. The author wishes to thank M. Tikanmäki, K. Kolari, and K. Kanervo for intriguing discussions and J. Kurkela, E. Schlesier, R. Mahlberg, and S. Takala for preparing the figures.

[1] D. Chandler, "Interfaces and the driving force of hydrophobic assembly," Nature **437**, 640–647 (2005).
[2] Y. Zheng, H. Bai, Z. Huang, X. Tian, F.-Q. Nie, Y. Zhao, J. Zhai, and L. Jiang, "Directional water collection on wetted spider silk," Nature **463**, 640–643 (2010).
[3] P. G. de Gennes, F. Brochard-Wyart, and D. Quéré, *Capillarity and Wetting Phenomena* (Springer, 2004).
[4] S. Shibuichi, T. Onda, N. Satoh, and K. Tsujii, "Super water-repellent surfaces resulting from fractal surfaces," J. Phys. Chem. **100**, 19512–19517 (1996).
[5] A. Lafuma and D. Quéré, "Superhydrophobic states," Nat. Mater. **2**, 457–460 (2003).
[6] T. Young, "An essay on the cohesion of fluids," Philos. Trans. R. Soc. London **95**, 65 (1805).
[7] W. A. Zisman, "Relation of the equilibrium contact angle to liquid and solid constitution," in *Contact Angle, Wettability, and Adhesion*, Advances in Chemistry (Wiley, 1964), Chap. 1, Vol. 43, pp. 1–51.
[8] P. G. de Gennes, "Wetting: Statistics and dynamics," Rev. Mod. Phys. **57**, 827–863 (1985).
[9] B. Krasovitski and A. Marmur, "Drops down the hill: Theoretical study of limiting contact angles and the hysteresis range on a tilted plane," Langmuir **21**, 3881–3885 (2005).
[10] E. Bormashenko, *Wetting of Real Surfaces* (de Gruyter, Berlin, 2013).
[11] C. G. L. Furmidge, "Studies at phase interfaces," J. Colloid Sci. **17**, 309–324 (1962).
[12] H. B. Eral, D. J. C. M. 't Mannetje, and J. M. Oh, "Contact angle hysteresis: A review of fundamentals and applications," Colloid Polym. Sci. **291**, 247–260 (2013).
[13] V. Starov, "Static contact angle hysteresis on smooth, homogenous solid substrates," Colloid Polym. Sci. **291**, 261–270 (2013).
[14] I. Kuchin and V. Starov, "Hysteresis of contact angle of sessile droplets on smooth homogeneous solid substrates via disjoining/conjoining pressure," Langmuir **31**, 5345–5352 (2015).
[15] I. V. Kuchin and V. M. Starov, "Hysteresis of the contact angle of a meniscus inside a capillary with smooth, homogeneous solid walls," Langmuir **32**, 5333–5340 (2016).
[16] S. Vedantam and M. V. Panchagnula, "Constitutive modeling of contact angle hysteresis," J. Colloid Interface Sci. **321**, 393–400 (2008).
[17] P. Rahimi and C. A. Ward, "Contact angle hysteresis on smooth and homogenous surfaces in gravitational fields," Microgravity Sci. Technol. **16**, 231–235 (2005).
[18] R. J. Hunter, *Foundations of Colloid Science* (Clarendon, Oxford, 1995).
[19] I. B. Ivanov, P. A. Kralchevsky, and A. D. Nikolov, "Film and line tension effects on the attachment of particles to an interface: I. Conditions for mechanical equilibrium of fluid and solid particles at a fluid interface," J. Colloid Interface Sci. **112**, 97–107 (1986).
[20] L. Makkonen, "Misinterpretation of the Shuttleworth equation," Scri. Mater. **66**, 627–629 (2012).
[21] L. Makkonen, "Young's equation revisited," J. Phys.: Condens. Matter **28**, 135001 (2016).
[22] J. F. Joanny and P. G. de Gennes, "A model for contact angle hysteresis," J. Chem. Phys. **81**, 552–562 (1984).
[23] R. Lhermerout, H. Perrin, E. Rolley, B. Andreotti, and K. Davitt, "A moving contact line as a rheometer for nanometric interfacial layers," Nat. Commun. **7**, 12545 (2016).
[24] D. Berthelot, Compt. Rendus **126**, 1703–1706 (1898).
[25] D. Y. Kwok and A. W. Neumann, "Contact angle interpretation in terms of solid surface tension," Colloids Surf., A **161**, 31–48 (2000).
[26] J. Lyklema, "The surface tension of pure liquids: Thermodynamic components and corresponding states," Colloids Surf., A **156**, 413–421 (1999).
[27] L. A. Girifalco and R. J. Good, "A theory for the estimation of surface and interfacial energies. I. Derivation and application to interfacial tension," J. Phys. Chem. **61**, 904–909 (1957).
[28] B. Janczuk, J. M. Bruque, M. L. Gonzales-Martin, J. Moreno del Pozo, A. Zdziennicka, and F. Quintana-Gragera, "The usefulness of the equation of state for interfacial tensions estimation in some liquid-liquid and solid-liquid systems," J. Colloid Interface Sci. **181**, 108–117 (1996).
[29] A. W. Neumann, R. J. Good, C. J. Hope, and M. Seijpal, "An equation-of-state approach to determine surface tensions of low-energy solids from contact angles," J. Colloid Interface Sci. **49**, 291 (1974).
[30] H. Tavana and A. W. Neumann, "On the question of rate-dependence of contact angles," Colloids Surf., A **282-283**, 256–262 (2006).

[31]J. V. I. Timonen, M. Latikka, O. Ikkala, and R. H. A. Ras, "Free-decay and resonant methods for investigating the fundamental limit of superhydrophobicity," Nat. Commun. **4**, 2398 (2013).
[32]M. Miyama, Y. Yang, T. Yasuda, T. Okuno, and H. K. Yasuda, "Static and dynamic contact angles of water on polymeric surfaces," Langmuir **13**, 5494–5503 (1997).
[33]R. Dufour, M. Harnois, V. Thomy, R. Boukherroub, and V. Senez, "Contact angle hysteresis origins: Investigation on super-omniphobic surfaces," Soft Matter **7**, 9380–9387 (2011).
[34]C. Satriano, G. Marletta, S. Guglielmino, and S. Carnazza, "Cell adhesion to ion- and plasma-treated polymer surfaces: The role of surface free energy," in *Contact Angle, Wettability and Adhesion* (Wiley, 2006), Vol. 4, pp. 471–486.
[35]F. J. Montes Ruiz-Cabello, M. A. Rodriguez-Valverde, and M. Cabrerizo-Vilchez, "A new method for evaluating the most stable contact angle using tilted plate experiments," Soft Matter **7**, 10457 (2011).
[36]N. R. Morrow, "The effects of surface roughness on contact angle with special reference to petroleum recovery," J. Can. Pet. Technol. **14**, 42–53 (1975).
[37]H. Y. Erbil, G. McHale, S. M. Rowan, and M. I. Newton, "Determination of the receding contact angle of sessile drops on polymer surfaces by evaporation," Langmuir **15**, 7378–7385 (1999).
[38]E. Pierce, F. J. Carmona, and A. Amirfazli, "Understanding of sliding contact angle results in tilted plane experiments," Colloids Surf., A **323**, 73–82 (2008).
[39]E. Bormashenko, Y. Bormashenko, G. Whyman, R. Pogreb, A. Musin, R. Jager, and Z. Barkay, "Contact angle hysteresis on polymer substrates established with various experimental techniques, its interpretation, and quantitative characterization," Langmuir **24**, 4020–4025 (2008).
[40]J. T. Korhonen, T. Huhtamäki, O. Ikkala, and R. H. A. Ras, "Reliable measurement of the receding contact angle," Langmuir **29**, 3858–3863 (2013).
[41]D. Quere, "Wetting and roughness," Annu. Rev. Mater. Res. **38**, 71–99 (2008).
[42]H. Kamusewitz, W. Possart, and D. Paul, "The relation between Young's equilibrium contact angle and the hysteresis on rough paraffin wax surfaces," Colloids Surf., A **156**, 271–279 (1999).
[43]E. Bormashenko, "Physics of solid-liquid interfaces: From the Young equation to the superhydrophobicity," Low Temp. Phys. **42**, 622–635 (2016).
[44]A. Marmur, "Solid-surface characterization by wetting," Annu. Rev. Mater. Res. **39**, 473–489 (2009).
[45]K. Y. Yeh, L. J. Chen, and J. Y. Chang, "Contact angle hysteresis on regular pillar-like hydrophobic surfaces," Langmuir **24**, 245–251 (2008).
[46]W. Choi, A. Tuteja, J. M. Marby, R. E. Cohen, and G. H. McKinley, "A modified Cassie–Baxter relationship to explain contact angle hysteresis and anisotropy on non-wetting textured surfaces," J. Colloid Interface Sci. **339**, 208–216 (2009).
[47]B. M. L. Koch, A. Amirfazli, and J. A. W. Elliott, "Modeling and measurement of contact angle hysteresis on textured high-contact-angle surfaces," J. Phys. Chem. C **118**, 18554–18563 (2014).
[48]N. K. Adam and G. Jessop, "Angles of contact and polarity of solid surfaces," J. Chem. Soc., Trans. **127**, 1863–1868 (1925).
[49]M. J. Santos and J. A. White, "Theory and simulation of angular hysteresis on planar surfaces," Langmuir **27**, 14868–14875 (2011).
[50]T. L. Liu, Z. Chen, and C.-J. Kim, "A dynamic Cassie-Baxter model," Soft Matter **11**, 1589–1596 (2015).
[51]M. Schmitt, R. Hempelmann, and F. Heib, "Experimental investigation of dynamic contact angles on horizontal and inclined surfaces, Part I: Flat silicon oxide surfaces," Z. Phys. Chem. **228**, 11–25 (2014).
[52]A. Carlson, G. Bellani, and G. Amberg, "Contact line dissipation in short-time dynamic wetting," Europhys. Lett. **97**, 44004 (2012).
[53]L. Makkonen, "A thermodynamic model of sliding friction," AIP Adv. **2**, 012179 (2012).
[54]E. L. Decker, B. Frank, Y. Suo, and S. Garoff, "Physics of contact angle measurement," Colloids Surf., A **156**, 177–189 (1999).
[55]C. Andrieu, C. Sykes, and F. Brochard, "Average spreading parameter on heterogeneous surfaces," Langmuir **10**, 2077–2080 (1994).
[56]R. Tadmor, "Line energy and the relation between advancing, receding, and Young contact angles," Langmuir **20**, 7659–7664 (2004).
[57]M. J. Santos, S. Velasco, and J. A. White, "Simulation analysis of contact angles and retention forces on liquid drops on inclined surfaces," Langmuir **28**, 11819–11826 (2012).
[58]M. Dirany, L. Dies, F. Restagno, L. Léger, C. Poulard, and G. Miquelard-Garnier, "Chemical modification of PDMS surface without impacting the viscoelasticity: Model systems for a better understanding of elastomer/elastomer adhesion and friction," Colloids Surf., A **468**, 174–183 (2015).
[59]N. Belman, K. Jin, Y. Golan, J. N. Israelachvili, and N. S. Pesika, "Origin of the contact angle hysteresis of water on chemisorbed and physisorbed self-assembled monolayers," Langmuir **28**, 14609–14617 (2012).
[60]K. L. Cho, A. H. F. Wu, I. I. Liaw, D. Cookson, and R. N. Lamb, "Wetting transitions on hierarchical surfaces," J. Phys. Chem. C **116**, 26810–26815 (2012).
[61]R. Ramachandran, K. Sobolev, and M. Nosonovsky, "Dynamics of droplet impact on hydrophobic/icephobic concrete with the potential for superhydrophobicity," Langmuir **31**, 1437–1444 (2015).
[62]E. Chibowski, A. Ontiveros-Ortega, and R. Perea-Carpio, "On the interpretation of contact angle hysteresis," J. Adhes. Sci. Technol. **16**, 1367–1404 (2002).
[63]R. E. Johnson, R. E. Dettre, and D. A. Brandreth, "Dynamic contact angles and contact angle hysteresis," J. Colloid Interface Sci. **62**, 205–212 (1977).
[64]R. David and A. W. Neumann, "Contact angle patterns on low-energy surfaces," Adv. Colloid Interface Sci. **206**, 46–56 (2014).
[65]J.-H. Kim, H. P. Kavehpour, and J. P. Rothstein, "Dynamic contact angle measurements on superhydrophobic surfaces," Phys. Fluids **27**, 032107 (2015).
[66]D. Fell, G. Auernhammer, E. Bonaccurso, C. Liu, R. Sokuler, and H.-J. Butt, "Influence of surfactant concentration and background salt on forced dynamic wetting and dewetting," Langmuir **27**, 2112–2117 (2011).
[67]M. Schmitt, K. Gross, J. Grub, and F. Heib, "Detailed statistical contact angle analyses: 'Slow moving' drops on inclining silicon-oxide surfaces," J. Colloid Interface Sci. **447**, 229–239 (2015).
[68]C. N. C. Lam, R. Wu, D. Li, M. L. Hair, and A. W. Neumann, "Study of the advancing and receding contact angles: Liquid sorption as a cause of contact angle hysteresis," Adv. Colloid Interface Sci. **96**, 169–191 (2002).
[69]L. Boinovich and A. Emelyanenko, "Wetting and surface forces," Adv. Colloid Interface Sci. **165**, 60–69 (2011).
[70]E. L. Decker and S. Garoff, "Using vibrational noise to probe energy barriers producing contact angle hysteresis," Langmuir **12**, 2100–2110 (1996).
[71]L. M. Lander, L. M. Siewierski, W. J. Brittain, and E. A. Vogler, "A systematic comparison of contact angle methods," Langmuir **9**, 2237–2239 (1993).
[72]A. I. ElSherbini and A. M. Jacobi, "Retention forces and contact angles for critical liquid drops on non-horizontal surfaces," J. Colloid Interface Sci. **299**, 841–849 (2006).
[73]C. W. Extrand, "An experimental study on contact angle hysteresis," J. Colloid Interface Sci. **191**, 378–383 (1997).
[74]A. Carre, J. C. Gastel, and M. E. R. Shanahan, "Viscoelastic effects in the spreading of liquids," Nature **379**, 432–434 (1996).
[75]R. Tadmor, P. Bahadur, A. Leh, H. E. N'guessan, R. Jaini, and L. Dang, "Measurement of lateral adhesion forces at the interface between a liquid drop and a substrate," Phys. Rev. Lett. **103**, 266101 (2009).
[76]R. Tadmor, "Approaches in wetting phenomena," Soft Matter **7**, 1577–1580 (2011).
[77]H. E. N'guessan, A. Leh, P. Cox, P. Bahadur, R. Tadmor, P. Patra, R. Vajtai, P. M. Ajayan, and P. Wasnik, "Water tribology on graphene," Nat. Commun. **3**, 1242 (2012).
[78]R. Tran, Z. Xu, B. Radhakrishnan, D. Winston, W. Sun, K. A. Persson, and S. P. Onga, "Surface energies of elemental crystals," Sci. Data **3**, 160080 (2016).
[79]C. Lv and P. Hao, "Driving droplet by scale effect on microstructured hydrophobic surfaces," Langmuir **28**, 16958–16965 (2012).
[80]V. Hisler, L. Vonna, V. Le Houreu, S. Knopf, C. Gauthier, M. Nardin, and H. Haidara, "Model experimental study of scale invariant wetting behaviors in Cassie-Baxter and Wenzel regimes," Langmuir **30**, 9378–9383 (2014).